
Empowering Counterfactual Reasoning over Graph Neural Networks through Inductivity

Samidha Verma

Indian Institute of Technology, Delhi, India
samidha.verma@cse.iitd.ac.in

Burouj Armgaan

Indian Institute of Technology, Delhi, India
Burouj.Armgaan@cse.iitd.ac.in

Sourav Medya

University of Illinois, Chicago, USA
medya@uic.edu

Sayan Ranu

Indian Institute of Technology, Delhi, India
sayanranu@iitd.ac.in

Abstract

Graph neural networks (GNNs) have various practical applications, such as drug discovery, recommendation engines, and chip design. However, GNNs lack transparency as they cannot provide understandable explanations for their predictions. To address this issue, counterfactual reasoning is used. The main goal is to make minimal changes to the input graph of a GNN in order to alter its prediction. While several algorithms have been proposed for counterfactual explanations of GNNs, most of them have two main drawbacks. Firstly, they only consider edge deletions as perturbations. Secondly, the counterfactual explanation models are transductive, meaning they do not generalize to unseen data. In this study, we introduce an inductive algorithm called INDUCE, which overcomes these limitations. By conducting extensive experiments on several datasets, we demonstrate that incorporating edge additions leads to better counterfactual results compared to the existing methods. Moreover, the inductive modeling approach allows INDUCE to directly predict counterfactual perturbations without requiring instance-specific training. This results in significant computational speed improvements compared to baseline methods and enables scalable counterfactual analysis for GNNs.

1 Introduction and Related Work

The applications of Graph Neural Networks (GNNs) have percolated beyond the academic community. GNNs have been used for drug discovery [20], designing chips [16], and recommendation engines [31]. Despite significant success in prediction accuracy, GNNs, like other deep learning based models, lack the ability to explain why a particular prediction was made. Explainability of a prediction model is important towards making it trust-worthy. In addition, it sheds light on potential flaws and generates insights on how to further refine a model.

Existing Works: At a high level, GNN explainers can be classified into the two groups of *instance-level* [32, 14, 18, 36, 7, 35, 13, 21, 12, 4, 1, 27] or *model-level* explanations [33]. Consistent with their nomenclature, instance-level explainers explain a specific input graph, whereas model-level explainers provide a high-level explanation in understanding general behaviour of the GNN model trained over a set of graphs. Recent research has also focused on global concept-based [30, 2] explainers that provide both model and instance-level explanations. Instance-level methods can broadly be grouped into two categories: *factual* reasoning [32, 14, 18, 36, 7, 35] and *counterfactual* reasoning [13, 21, 4, 1, 27]. Given the input graph and a GNN, factual reasoners seek to identify the smallest sub-graph that is sufficient to make the same prediction as on the entire input graph. Counterfactual reasoners, on the other hand, seek to identify the smallest perturbation on the input data that changes the GNN's prediction. Perturbations correspond to removal and addition of edges.

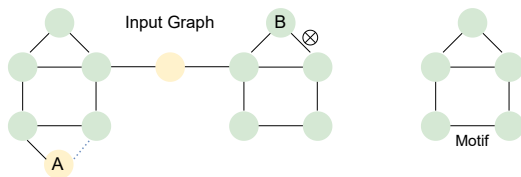


Figure 1: The figure contains two graphs with the right graph being labeled “Motif”. Each node in the left graph belongs to either the green class (label) or yellow. Green class indicates a node that is part of a subgraph isomorphic to the motif; yellow otherwise. Addition of the dotted edge incident on node A changes its label from yellow to green since it becomes part of the motif.

Compared to factual reasoning, counterfactual reasoners have the additional advantage of providing a means for recourse [23]. For example, in drug discovery [8, 29], mutagenicity is an adverse property of a molecule that hampers its potential to become a drug [9]. While factual explainers can attribute the subgraph causing mutagenicity, counterfactual reasoners can identify this subgraph along with the changes that would make the molecule non-mutagenic.

In this work, we study counterfactual reasoning over GNNs towards node classification. To illustrate our problem, let us consider the input graph shown in Fig. 1. Here, each node belongs to the *green* class if it is part of the motif (subgraph) shown on the right. Otherwise, it belongs to the *yellow* class. The dotted edge on node A does not exist, for now. At this stage, if we ask the counterfactual reasoner to flip the label of node A, the best answer would be to add the dotted edge. Similarly, for node B, one possible answer would be to delete the edge marked with \otimes .

Existing works on counter-factual reasoning over GNNs suffer from two key limitations:

- **Ability to add edges:** Most of the existing techniques do not consider addition of edges (or nodes); they only consider edge removals. This limitation severely compromises the search space consisting of possible “changes” on the input graph. As an example, in Fig. 1, if we only consider deletions, it is impossible to flip the label of A.
- **Inductive modeling:** Existing techniques, with the exception of GEM [12], are transductive in nature, i.e., they cannot generate counterfactuals on unseen nodes. As an example, if the model is trained to generate counterfactuals on node v of graph G , it cannot be used to generate counterfactuals on another node u of G . Consequently, these transductive models need to be retrained on each node of an input graph. In contrast, an inductive model learns parameters from a train set of nodes, which in turn can be used to *predict* counterfactual on unseen nodes. In addition, an inductive model is robust to changes in the input graph due to external factors such as new friend connections in a social network, citations in a citation network, etc.

Table G in the Appendix presents a structured summary of the instance-level explainers.

Contributions: In this work, we develop INDUCE (Inductive Counter-factual Explanations), that addresses the above limitations of existing counterfactual reasoners. We propose INDUCE to address these challenges and make the following contributions:

- **Novel formulation:** We formulate the novel problem of *model-agnostic, inductive* counterfactual reasoning over GNNs for node classification. It is worth noting that both inductive modeling and the ability to add edges introduce non-trivial challenges. In inductive modeling, we need to learn parameters that embodies general rules to be used for predicting counterfactuals. In the transductive approach, since parameters are learned for each specific node, there is no generalization component. Edge additions introduce a significant scalability challenge as the number of possible additions grows quadratically to the number of nodes in the graph. In contrast, the number of edge deletions is $O(|\mathcal{E}|)$, where \mathcal{E} is the set of edges in the graph. (§ 2).
- **Algorithm:** Identifying the smallest number of edge additions or removals that alter the prediction is a combinatorial optimization problem. We prove that computing the optimal solution to the problem is NP-hard (§ 2). As a heuristic, we *learn* to solve this combinatorial optimization problem through reinforcement learning powered by *policy gradients* [28] (§ 3).
- **Empirical validation:** Through extensive experiments on benchmark graph datasets, we show that INDUCE outperforms state-of-the-art algorithms in metrics relevant to counterfactual reasoning. We further analyze the generated counterfactuals and provide compelling evidence that enabling edge additions is indeed the reason driving INDUCE’s superior performance. Finally, we also

showcase the computation gains obtained due to embracing the inductive paradigm instead of transductive modeling (§ 4).

2 Preliminaries and Problem Formulation

We use the notation $\mathcal{G} = (\mathcal{V}, \mathcal{E})$ to denote a graph with node set \mathcal{V} and edge set \mathcal{E} . We assume each node $v_i \in \mathcal{V}$ is characterized by a feature vector $x_i \in \mathbb{R}^d$. Furthermore, $l(v) : \mathcal{V} \rightarrow \mathcal{C}$ is a function mapping each node v to its true class label drawn from a set \mathcal{C} . We assume there exists a GNN Φ that has been trained on \mathcal{G} . Given an input node $v_i \in \mathcal{V}$, we assume $\Phi(\mathcal{G}, v, c)$ outputs a probability distribution over class labels $c \in \mathcal{C}$. The predicted class label is therefore the class with the highest probability, which we denote as $L_\Phi(\mathcal{G}, v) = \arg \max_{c \in \mathcal{C}} \{\Phi(\mathcal{G}, v, c)\}$.

Problem 1 (Counterfactual Reasoning on GNNs) *Given input graph $\mathcal{G} = (\mathcal{V}, \mathcal{E})$, a target node $v \in \mathcal{V}$, a GNN model Φ , and an optional set of node pairs $\mathcal{V}_c = \{(v_i, v_j) \mid v_i, v_j \in \mathcal{V}\}$ between which edges may be perturbed, find the closest graph \mathcal{G}^* by minimizing the number of perturbations, such that $L_\Phi(\mathcal{G}^*, v) \neq L_\Phi(\mathcal{G}, v)$ and all perturbed edges are among pairs in \mathcal{V}_c .*

In a real world, we may not have control over all perturbations. \mathcal{V}_c allows us to specify that. If $\mathcal{V}_c \subseteq \mathcal{E}$, we restrict to only deletions. On the other hand, if $\mathcal{V}_c \cap \mathcal{E} = \emptyset$, we only allow additions.

In our problem, we enforce two restrictions on the counterfactual reasoner. First, it should be *model-agnostic*, i.e., only the output of Φ is visible to us, but not its parameters. Second, the reasoner should be *inductive*, which means we should learn a *predictive model* Π , that can predict the counterfactual graph \mathcal{G}^* given the inputs \mathcal{G} , GNN Φ , and target node v .

Theorem 1 (NP-hardness) *Counterfactual reasoning for GNNs, i.e., Prob. 1, is NP-hard.*

We prove NP-hardness by mapping counter-factual reasoning over GNNs to the *set-cover* problem. The details are provided in the App. A). Owing to NP-hardness, it is not feasible to identify the closest counterfactual graph in polynomial time. Hence, we aim to design effective heuristics.

3 INDUCE

Our goal is to learn an inductive counterfactual reasoning model Π , and thus, the proposed algorithm is broken into two phases: *training* and *inference*. During training, we learn the parameters of the model Π and during inference, we predict the counterfactual graph using Π . Theorem 1 prohibits us from supervised learning since generating training data of ground-truth counterfactuals is NP-hard. Hence, we use reinforcement learning. Through *discounted rewards*, reinforcement learning allows us to model the combinatorial relationships [10] in the perturbation space.

3.1 Learning Π as an MDP

Given graph \mathcal{G} , we randomly select a subset of vertices from \mathcal{V} to train Π . Given a target node v , the task of Π is to iteratively delete or add edges such that with each perturbation the likelihood of $\Phi(\mathcal{G}^t, v) \neq \Phi(\mathcal{G}, v)$ changes maximally. Here, $\mathcal{G}^t = (\mathcal{V}, \mathcal{E}^t)$ denotes graph \mathcal{G} after t perturbations starting with $\mathcal{G}^0 = \mathcal{G}$. We model this task of iterative perturbations as a *markov decision process (MDP)*. Specifically, the *state* captures a latent representation of the graph indicative of how it would react to a perturbation. An *action* corresponds to an edge addition or deletion by Π . Finally, the *reward* is a function of the number of perturbations, which we want to minimize, and the probability of $\Phi(\mathcal{G}^t, v)$ flipping following the next action (edge addition or deletion), a value that we want to maximize. We next formalize each of these notions.

State: Intuitively, the state should characterize how likely the class label of the target node v would flip following a given action. Towards that end, we observe that a GNN of ℓ layers aggregates information from the ℓ -hop neighborhood of v . Nodes outside this neighborhood do not impact the prediction of a GNN. Motivated by this design of GNNs, the state in our problem is the set of node representations in the h -hop neighborhood of the target node v , where ideally $h > \ell$. Specifically, at time t , the state is:

$$\mathbf{S}_v^t = \{\mathbf{x}_u^t \mid u \in \mathcal{N}_v^h\}, \text{ where} \quad (1)$$

$$\mathcal{N}_v^h = \{u \in \mathcal{V} \mid sp(v, u) \leq h\} \quad (2)$$

Here, $sp(v, u)$ denotes the length of the shortest path from v to u in the original graph $\mathcal{G} = (\mathcal{V}, \mathcal{E})$.

The representations of nodes, i.e., \mathbf{x}_u^t , are constructed using a combination of semantic, topological, and statistical features.

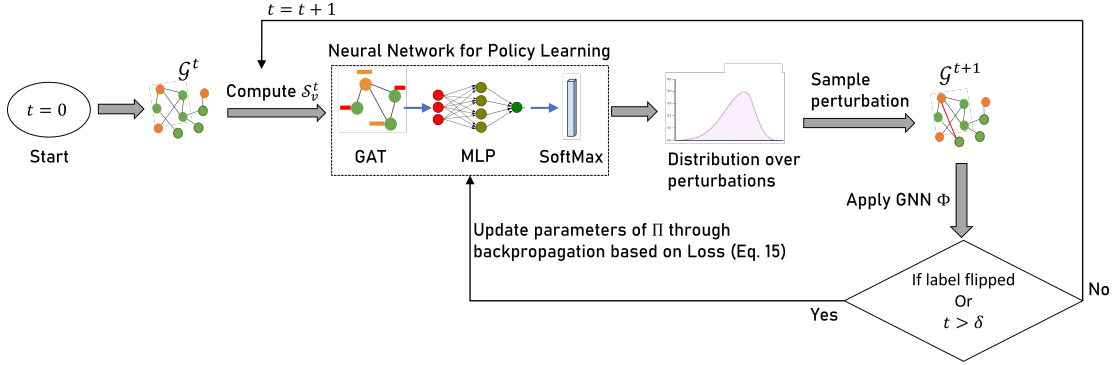


Figure 2: Pipeline of the policy learning algorithm in INDUCE. δ indicates the maximum number of allowed perturbations.

- *Original node Features*: It is common to encounter graphs where nodes are annotated with features or labels (recall the definition of x_i in § 2). We retain these features.
- *Degree Centrality*: The higher the degree of a node, the more information it receives from its neighbors. Thus, when an edge is added or deleted from the target node to a high-degree node, it may have significant impact on the representation of the target. Based on this observation, we use the degree of a node as a part its representation.
- *Entropy*: The entropy of a node at time t is defined as $e_u^t = -\sum_{c \in \mathcal{C}} p_c \log p_c$, where $p_c = \Phi(\mathcal{G}^t, v, c)$. The entropy quantifies the uncertainty of the GNN Φ on a given node. We hypothesize that if the Φ is highly certain (i.e., low entropy) about the class label of some node u , then any perturbation on u is unlikely to make it flip. Similarly, the opposite is true on nodes with high entropy. Due to this information content of entropy, we use it as one of the features in \mathbf{x}_u^t .
- *Class label*: Finally, we include the predicted class label of a node, i.e., $L_\Phi(\mathcal{G}^t, u)$ in the form of one-hot encodings of dimension \mathcal{C} .

The final representation of node u and time t is therefore the concatenation of the above features, i.e.,

$$\mathbf{x}_u^t = x_i \parallel degree_u^t \parallel e_u^t \parallel (\text{one-hot}(L_\Phi(\mathcal{G}^t, u))) \quad (3)$$

Here, \parallel represents the *concatenation* operator.

Actions: The action space consists of all possible edge deletions in the h -hop neighborhood of target node v and additions of edges from v to other non-attached nodes in its h -hop neighborhood. Formally, the sets are defined as follows:

$$\mathcal{E}_{v,del}^t = \{e = (u_i, u_j) \in \mathcal{E}^t \mid u_i, u_j \in \mathcal{N}_v^h\} \quad (4)$$

$$\mathcal{E}_{v,add}^t = \{e = (v, u_j) \notin \mathcal{E}^t \mid u_j \in \mathcal{N}_v^h\} \quad (5)$$

The action space is the perturbation set: $\mathcal{P}^t = \mathcal{E}_{v,del}^t \cup \mathcal{E}_{v,add}^t$ (6)

Reward: Our objective is to flip the predicted label of target node v with the minimum number of perturbations in \mathcal{N}_v^h in order to find the counterfactual. To capture these intricacies, we formulate the reward of an action a as a combination of the prediction accuracy of GNN Φ and the number of perturbations made so far.

$$\mathcal{R}_v^t(a) = \frac{1}{\mathcal{L}_{v,pred}^{t+1} + \beta \times d(\mathcal{G}, \mathcal{G}^t)}, \text{ where} \quad (7)$$

$$\mathcal{L}_{v,pred}^t = \sum_{c \in \mathcal{C}} \mathbb{1}_{l(v)=c} \log(\Phi(\mathcal{G}^t, v, c)), d(\mathcal{G}, \mathcal{G}^t) = t + 1 \quad (8)$$

In simple terms, $\mathcal{L}_{v,pred}^{t+1}$ is the *log-likelihood* of the data predicted by Φ in \mathcal{G}^{t+1} on v . \mathcal{G}^{t+1} is the created upon perturbing \mathcal{G}^t with action a . β is a hyper-parameter that regulates how much weight is given to log-likelihood of the data vs. the perturbation count. d is the distance function, which in our case is simply the number of edge edits made to \mathcal{G} at time step t .

State Transitions: At time t , the action corresponds to selecting a perturbation $a \in \mathcal{P}^t$ (Recall Eq. 6) from $p_{a,v}^t \sim \Pi(a \mid \mathcal{S}_v^t)$. We will discuss the computation of $p_{a,v}^t$ in § 3.2.

3.2 Neural Architecture for Policy Training

To learn $p_{a,v}^t$, we take the representations in \mathbf{S}_v^t , and pass them through a neural network comprising of a K -layered *Graph Attention Network* (GAT) [22], an MLP, and a final SoftMax layer.

The GAT learns a d -dimensional representation $\mathbf{a} \in \mathbb{R}^d$ for each perturbation $a \in \mathcal{P}_v^t$. \mathbf{a} is then passed through an *Multi-layered Perceptron (MLP)* to embed them into a scalar representing their value, which is finally passed over a *SoftMax* layer to learn a distribution over \mathcal{P}_v^t . The entire network is trained end-to-end. We next detail each of these components.

GAT: Let $\forall u \in \mathcal{N}_v^h, \mathbf{h}_u^0 = \mathbf{x}_u^t$ (Recall Eq.3). In each layer $k \in [1, K]$, we perform the following transformation:

$$\mathbf{h}_u^k = \sigma \left(\sum_{\forall u' \in \mathcal{N}_u^1 \cup \{u\}} \alpha_{u,u'}^k \mathbf{W}^k \mathbf{h}_{u'}^{k-1} \right) \quad (9)$$

σ is an activation function, $\alpha_{u,u'}^k$ are learnable, layer-specific attention weights, and $\mathbf{W}^k \in \mathbb{R}^{d^{k-1} \times d^k}$ is a learnable, layer-specific weight matrix where d^k is the hyper-parameter denoting the representation dimension in hidden layer k . In our implementation, we use LeakyReLU with negative slope 0.01 as the activation function. The attention weights are learned through an MLP followed by a *SoftMax* layer. Specifically,

$$e_{u,u'}^k = \text{MLP}(\mathbf{h}_u^{k-1} \parallel \mathbf{h}_{u'}^{k-1}), \text{ where } e_{u,u'}^k \in \mathbb{R}, \quad \alpha_{u,u'}^k = \frac{\exp(e_{u,u'}^k)}{\sum_{\hat{u} \in \mathcal{N}_u^1 \cup \{u\}} \exp(e_{u,\hat{u}}^k)}$$

After K layers, the GAT outputs the final representation $\mathcal{X}_u = \mathbf{h}_u^K$ for each node u in v 's neighborhood. Semantically, given the initial state representation \mathbf{x}_u^t , the GAT enriches them further by merging with topological information. Finally, the representation of an action $a \in \mathcal{P}_v^t$ is set to $\mathbf{a} = \mathcal{X}_u \parallel \mathcal{X}_v \parallel t(u, v)$, where:

$$t(u, v) = \begin{cases} 0, & a \in \mathcal{E}_{v,del}^t \text{ (Recall Eq. 4)} \\ 1, & a \in \mathcal{E}_{v,add}^t \text{ (Recall Eq. 5)} \end{cases} \quad (10)$$

MLP and SoftMax layers: The value of a is $s_a = \text{MLP}(\mathbf{a})$, where $s_a \in \mathbb{R}$. Finally, we get a distribution over all actions in \mathcal{P}_v^t as:

$$p_{a,v}^t = \Pi(a \mid \mathcal{S}_v^t) = \frac{\exp(s_a)}{\sum_{\forall a' \in \mathcal{P}_v^t} \exp(s_{a'})} \quad (11)$$

3.3 Policy Loss Computation

We iteratively sample an action as per Eq. 11 till either the label flips or we exceed the maximum number of perturbations (which is a hyper-parameter). This iterative selection generates a trajectory of perturbations $\mathcal{T}_v = \{a_1, \dots, a_m\}$. We use the standard loss for policy gradients on \mathcal{T}_v [28]. More specifically, we minimize the following loss function:

$$\mathcal{J}(\Pi) = -\frac{1}{\mathcal{V}_{tr}} \left(\sum_{\forall v \in \mathcal{V}_{tr}} \left(\sum_{t=0}^{|\mathcal{T}_v|} \log p_{a,v}^t \mathcal{R}_v^t(a_t) + \eta \text{Ent}(\mathcal{P}_v^t) \right) \right) \quad (12)$$

Here, $\mathcal{V}_{tr} \subseteq \mathcal{V}$ is the subset of nodes on which the RL policy is being trained. $\text{Ent}(\mathcal{P}_v^t)$ is the entropy of the current probability distribution over the action space.

$$\text{Ent}(\mathcal{P}_v^t) = - \sum_{\forall a \in \mathcal{P}_v^t} p_{a,v}^t \log(p_{a,v}^t) \quad (13)$$

By adding the entropy to the loss, we encourage the RL agent to explore when there is high uncertainty. η is a hyper-parameter balancing the *explore-exploit* trade-off. For simplicity of exposition, we omit the discussion on discounted rewards in Eq. 12. Discounted rewards better capture the combinatorial relationship in the perturbation space. Refer to App. B for details.

3.4 Training and Inference

Fig. 2 presents the training pipeline. Starting from the original graph, we compute the state representation at each iteration t . The state is passed to the neural network to compute a distribution over the perturbation space. A perturbation is sampled from this distribution and the graph is accordingly modified. The GNN ϕ is then applied on the modified graph. If the label flips or the number of perturbation exceeds the maximum limit, we update the policy parameters. Otherwise,

Table 1: The statistics of the benchmark datasets.

	Tree-Cycles	Tree-Grid	BA-Shapes	Amazon	ogbn-arxiv
# Classes	2	2	4	6	40
# Nodes	871	1231	700	397	169,343
# Edges	1950	3410	4100	2700	1,166,243
Motif size (# nodes)	6	9	5	NA	NA
Motif size (# edges)	6	12	6	NA	NA
# Nodes from motifs	360	720	400	NA	NA
Avg node degree	2.23	2.77	5.86	15.90	6.89

we update the state and continue building the perturbation trajectory in the same manner. The pseudocode of the training pipeline is provided in Alg.1 in the Appendix.

Inductive inference: We iteratively make forward passes till the label flips or we exceed the budget. The forward pass is identical to the training phase with the only exception being we deterministically choose the perturbation with the highest likelihood instead of sampling.

Transductive Inference: This phase proceeds identical to the training phase with the only exception that we learn a target node specific policy instead of one that generalizes across all nodes.

Complexity of INDUCE: The time complexity of training phase is $\mathcal{O}(|\mathcal{V}_{tr}|(|\mathcal{V}| + |\mathcal{E}|))$ and the test phase is $\mathcal{O}(|\mathcal{V}_{test}|(|\mathcal{V}| + |\mathcal{E}|))$. Here \mathcal{V}_{tr} and \mathcal{V}_{test} denote the number of nodes in the train and test sets respectively. The derivations are provided in App. E.

4 Experiments

In this section, we benchmark INDUCE against established baselines. The code base and datasets used in our evaluation are available anonymously at <https://github.com/idea-iitd/Induce.git>. Details of the hardware and software platform are provided in App. F.

4.1 Datasets

Benchmark Datasets: We use the same three benchmark graph datasets used in [21, 12, 13]. Statistics of these datasets are listed in Table 1. Each dataset has an undirected base graph with pre-defined motifs attached to random nodes of the base graph, and randomly added additional edges to the overall graph. The class label of a node indicates whether it is part of a node or not. Further details on the datasets are provided in App. F.1.

- **Real Dataset:** We additionally use real-world datasets from the Amazon-photos co-purchase network [19] and ogbn-arxiv [25]. In the Amazon dataset, each node corresponds to a product, edges correspond to products that are frequently co-purchased, node features encode bag-of-words from product reviews and the node class label indicates the product category. The ogbn-arxiv dataset is a citation network. The nodes are all computer science arXiv papers indexed by MAG [25]. Each directed edge represents that one paper cites another. The features are word embeddings of the title and the abstract computed by the skip-gram model [15]. The labels are subject areas. Since the class labels in these datasets are not based on presence or absence of motifs, the corresponding cells in Table 1 are marked as “NA”.

4.2 Baselines

We benchmark INDUCE against the state-of-the-art baselines of (1) CF-GNNEXPLAINER [13], (2) CF² [21], and (3) GEM [12]. In addition, we also compare against the state-of-the-art factual explainer (4) PGEXPLAINER to show that when factual explainers are used for counter-factual reasoning by removing the factual explanation (subgraph) from the input graph, they are not effective. This is consistent with prior reported literature [13, 21, 12]. Finally, we also compare against (5) RANDOM perturbations. While CF² and CF-GNNEXPLAINER are transductive, GEM and PGEXPLAINER are inductive. The codebase of all algorithms have been obtained from the respective authors.

We do not consider [34] and [4] since they are limited to graph classification. We omit GNNEXPLAINER[32], since both CF² and CF-GNNEXPLAINER outperformed GNNEXPLAINER. Further, we do not study Bacciu et al. [3] since it uses internal representations of the black-box GNN model to exploit domain-specific knowledge. We focus on a domain-agnostic setting. Furthermore, unlike in

Method	Tree-Cycles			Tree-Grid			BA-Shapes		
	Fid.(%) ↓	Size ↓	Acc.(%) ↑	Fid.(%) ↓	Size ↓	Acc.(%) ↑	Fid.(%) ↓	Size ↓	Acc.(%) ↑
RANDOM	0	3.18 ±2.32	67.08	0	8.32 ±4.95	73.44	0	283.97 ±272.76	15.57
CF-GNNEX	49.0	1.05 ±0.23	100	10	1.37 ±0.58	92.24	37.0	1.31 ±0.55	95.83
CF ²	76.38	4.18 ±1.89	67.68	98.45	5.5 ±1.5	44.64	23.68	4.10 ±1.64	70.54
INDUCE (transductive)	0	1.01 ±0.12	98.61	0	1.02 ±0.12	97.67	0	1.30 ±0.90	95.31
CF-GNNEX ++	100	NULL	NULL	100	NULL	NULL	38.16	6315.44 ±9916.50	17.36
CF ² ++	13.89	28.34 ±7.56	19.24	28.68	12.90 ±7.71	27.44	100	NULL	NULL
INDUCE (transductive) --	0	1.40 ±1.49	81.94	0	1.24 ±0.43	92.64	6.6	1.42 ±1.49	83.22

Table 2: **Results for transductive methods:** Lower fidelity, smaller size, and higher accuracy are desired. The best results are highlighted in bold. Fid. denotes fidelity and Acc. denotes Accuracy.

Method	Tree-Cycles			Tree-Grid			BA-Shapes		
	Fid.(%) ↓	Size ↓	Acc.(%) ↑	Fid.(%) ↓	Size ↓	Acc.(%) ↑	Fid.(%) ↓	Size ↓	Acc.(%) ↑
PGEXPLAINER	34.72	6	76.85	41.09	6	66.93	6.58	6	89.25
GEM	95	6	88.97	97	6	94.57	17	6	98.44
INDUCE (inductive)	0	2.31 ±1.44	96.65	0	4.67 ±2.91	91.05	2.6	4.37 ±3.53	64.40
INDUCE (inductive) --	36.3	1.67 ± 0.90	90.32	16.3	6.38 ±3.74	86.31	40.8	3.37 ±3.04	56.08

Table 3: **Results for inductive methods.** The best result in each category is highlighted in bold.

[3], we do not assume access to the embeddings of the black-box model. Hence, our algorithm is also applicable in situations where the internal details of the GNN are hidden from the end-user due to proprietary reasons.

4.2.1 Performance measures

To quantify performance, we use the standard measures from the literature [13].

- **Fidelity:** Fidelity is the percentage of nodes whose labels do not change when the edges produced by the explainer (algorithm) are perturbed. Lower fidelity is better. Furthermore, it may be argued that fidelity is the most important metric among the three measures.
- **Size:** Explanation size is the number of edges perturbed for a given node. Lower size is better.
- **Accuracy:** Accuracy is the percentage of explanations that are correct. As standard in CF², CF-GNNEXPLAINER, and GEM, this translates to the percentage of edges in the counterfactual that belong to the motif. Since nodes have a non-zero class label only if they belong to a motif, the explanation for nodes should be edges in the motif itself. Note that accuracy is computable only on the benchmark datasets since they include ground-truth explanations.
- **Sparsity:** Sparsity is defined as the proportion of edges from \mathcal{N}_v^ℓ , i.e., the ℓ -hop neighbourhood of the target node, that is retained in the counter-factual v [35]; a value close to 1 is desired. Since sparsity is inversely correlated to size, we present sparsity values of our experiments in App. G.

Other settings: Details of additional experimental settings regarding the counterfactual task, the black-box GNN, training and inference are given in App. F.3.

4.3 Quantitative Results on Benchmark Datasets

Transductive methods: Table 2 presents the results (for now, we will focus on the first four rows). Our method INDUCE in the transductive setting outperforms all the baselines almost in all settings. For Tree-Cycles and BA-Shapes, CF-GNNEXPLAINER is producing better accuracy. However, we note that its fidelity is much worse, indicating it fails to find an explanation more frequently. More generally, while CF-GNNEXPLAINER consistently achieves the lowest size among the baselines, its fidelity is much worse. This indicates that CF-GNNEXPLAINER is able to solve only the easy cases and hence the low size is deceptive as it did not solve the difficult ones.

Inductive methods: Table 3 shows that INDUCE is superior to GEM and PGEXPLAINER in most cases. The fidelity scores produced by GEM and PGEXPLAINER are much higher (worse). This indicates, in most of the cases, GEM and PGEXPLAINER are unable to find a counterfactual example. Also recall that the explanation size is fixed in GEM and PGEXPLAINER since they work with fixed budgets. **Transductive vs Inductive:** We further compare the inductive version (Table 3) of our method, INDUCE with the transductive baselines (Table 2). While the transductive methods have a clear

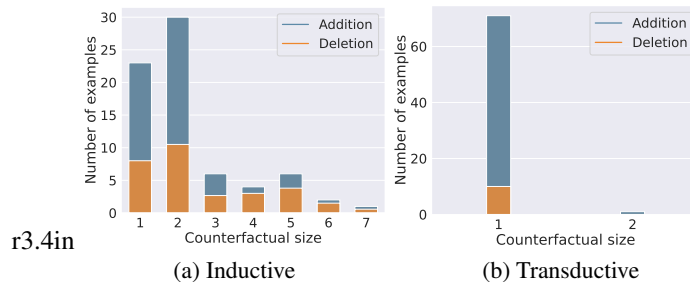


Figure 3: The distributions of the edit size and their internal composition of edge additions and deletions by INDUCE on the Tree-Cycles dataset.

advantage of re-training the model instance wise, the results produced by INDUCE-inductive are comparable. As noted earlier, although CF-GNNEXPLAINER achieves better size than INDUCE-inductive, its fidelity is much worse indicating that the low size is a manifestation of not being able to explain the hard cases that INDUCE is able to explain. Moreover, in addition to the ability to generalize to unseen nodes, inductive modeling also imparts a dramatic speed-up in generating explanations (see Table 6a).

Impact of edge additions: We seek answers to two key questions: **(1)** How much does the performance of INDUCE deteriorate if we restrict edge additions? **(2)** If we empower the baselines also with additions, do they match up to INDUCE? To answer the first question, we study the performance of INDUCE in the setting where only edge deletions are allowed. The rows corresponding to INDUCE (transductive)—— and INDUCE (inductive)—— in Tables 2 and 3 present these results. It is evident that the deletion-only version produces inferior results for both the transductive and inductive versions. In Fig. 3, we further study the frequency distribution of edge additions and deletions in the counter-factual explanations produced by INDUCE in Tree-Cycles dataset (results on other datasets are in App. I). We observe that additions dominate the perturbations, and thereby, further establishing its importance, which INDUCE unleashes.

To address the second question, we empower CF-GNNEXPLAINER and CF² with edge additions, denoted as CF-GNNEXPLAINER ++ and CF² ++ respectively.¹ Both CF² and CF-GNNEXPLAINER use a *mask-based* strategy. A mask is a learnable binary matrix of the same dimension as the ℓ -hop neighborhood of the target node. By taking an element-wise product of the mask with the adjacency matrix, one obtains the edges to be deleted. When empowered with additions, the mask itself becomes the new adjacency matrix. Surprisingly, the performance of CF-GNNEXPLAINER drops, while for CF², we see improvement in fidelity in two out of three datasets. Further investigation into this performance reveals that edge additions significantly increase the search space of possible perturbations (See Table H in Appendix). A mask-based strategy is a single-shot learnable paradigm that does not examine the marginal effect of each perturbation. When the perturbation space increases, it overwhelms the learning procedure. In contrast, INDUCE uses reinforcement learning where a trajectory of perturbations is selected based on their marginal gains. This allows better modeling of the combinatorial nature of counter-factual reasoning.

Overall, the above experiments reveal that both additions, as well as an algorithm equipped to model large combinatorial spaces, are required to perform well.

Additional experiments: App. H contains further empirical data on **(1)** the impact of heuristic features and **(2)** the choice of GNN architecture in the MDP on performance. Experiments on counterfactual size vs accuracy trade-off are given in App. J.

4.4 Quantitative Results on Real Datasets

In Tables 4a and 4b, we present the results. Consistent with the performance on benchmark datasets, INDUCE continues to outperform all the baselines almost in both transductive and inductive settings. We note that most of the baselines failed to produce counterfactuals in Amazon. In ogbn-arxiv, on the other hand, all baselines except PGEXPLAINER fails to scale; they crash with out-of-memory

¹GEM is not extendible to additions (See App. F.2 for details), PGEXPLAINER does not incorporate perturbations with the intent of flipping the label since it is a factual explainer.

Method	Fid.(%) ↓	Size ↓	Method	Fidelity(%) ↓	Size ↓
RANDOM	100	NULL	PGEXPLAINER	100	NULL
CF-GNNEXPLAINER	100	NULL	GEM	100	NULL
CF ²	60	13.7 ± 16.98	INDUCE (inductive)	93.00	6.60 ± 2.87
INDUCE (transductive)	53.50	4.72 ± 4.38			

(a) Transductive

(b) Inductive

Table 4: Results for (a) transductive and (b) inductive methods on the Amazon dataset. “NULL” denotes that the method could not produce a counterfactual.

Method	Fid.(%) ↓	Size ↓	Method	Fidelity(%) ↓	Size ↓
CF-GNNEXPLAINER	DNS	DNS	PGEXPLAINER	95.50	4
CF ²	DNS	DNS	GEM	DNS	DNS
INDUCE (transductive)	0	1.00 ± 0.00	INDUCE (inductive)	78.7	3.11 ± 3.04

(a) Transductive

(b) Inductive

Table 5: Results for (a) transductive and (b) inductive methods on the ogbn-arxiv dataset. “DNS” denotes that the method could not produce a counterfactual as it did not scale. Refer to App. K that details reasons on why these baselines failed to scale on ogbn-arxiv.”

exception. In contrast, INDUCE produces promising performance with the transductive version achieving 0% fidelity.

4.5 Efficiency

Table 6a presents the inference times of various algorithms. First, the inductive methods (INDUCE, PGEXPLAINER and GEM) are much faster than the others. Between the inductive methods, PGEXPLAINER is the fastest. INDUCE-inductive is slower since the search space for INDUCE is larger due to accounting for both edge additions and deletions. Second, INDUCE-inductive is up to 79 times faster than the transductive methods such as CF-GNNEXPLAINER and CF². This speed-up is a result of only doing forward passes through the neural policy network, whereas, transductive methods learn the model parameters on each node separately. Even the transductive version of INDUCE is faster than the other transductive methods for Tree-Cycles and Tree-Grid.

Scalability against graph size: Table 6b presents the inference time per node across all datasets. We observe that INDUCE scales to million-sized networks such as ogbn-arxiv. We observe that the growth of the running time is closely correlated with the neighbourhood density, i.e., the average degree of the graph, and not the graph size. In a GNN with ℓ layers, only the ℓ -hop neighborhood of the target node matters.

4.6 Case Study: Counter-factual Visualization

In this section, we visually showcase how counter-factual explanations reveal vulnerabilities of GNNs and why edge additions are important.

Revealing GNN vulnerabilities: A sample counterfactual explanation by various algorithms on Tree-Cycles dataset is provided in Fig. 4a. The target node is part of a motif (6-cycle) and therefore the expected counter-factual explanation is to make it a non-member of a 6-cycle. CF-GNNEXPLAINER correctly finds on such explanation by deleting an edge. Both GEM and CF² recommend a much larger explanation than necessary. In contrast, INDUCE adds an edge. More interestingly, the target node continues to remain part of the motif. This uncovers a limitation of GNN since it falsely classifies the target node as a non-motif node although it is not. Furthermore, this limitation is uncovered only since INDUCE can add edges. Similar observations in other datasets are available in Figs. Ea-Eb in Appendix.

Impact of additions: In Fig. 4b top-left, we share an example where INDUCE flips the label of a target node (orange) by making it part of the 6-node cycle motif through edge addition. Since baseline strategies are only capable of deletes, they fail to flip the label of such nodes. Further in the top-right (Tree-Grid) example, we see INDUCE breaks the grid motif and connects the target node (orange) to a non-motif neighbour, hence colluding its embeddings and flipping its label. These examples showcase the importance of edge addition to intuitively explain how the black-box GNN works.

5 Conclusion

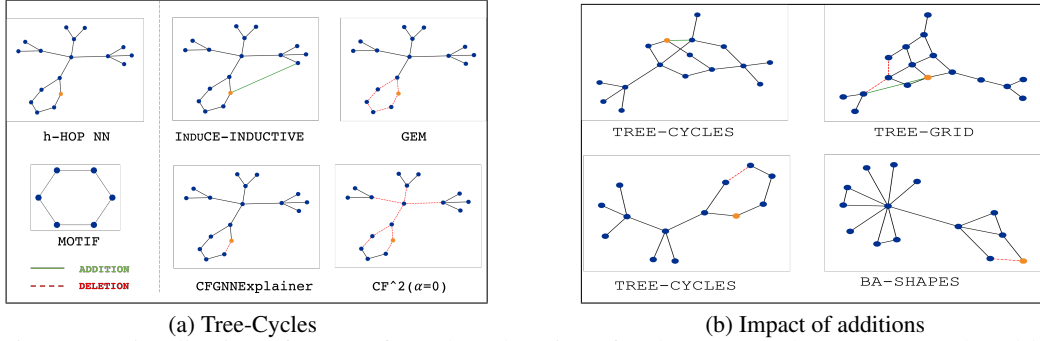
The ability to explain predictions is critical towards making a model trustworthy. In this work, we proposed INDUCE to understand GNNs via counterfactual reasoning for the node classification task. While several algorithms in the literature produce counterfactual explanations of GNNs, they suffer from restricted counterfactual space exploration and transductivity. INDUCE provides a boost to counterfactual analysis on GNNs by unleashing the power of edge additions and inductively predicting

Method	Tree-Cycles	Tree-Grid	BA-Shapes	Dataset	#Nodes	#Edges	Avg. degree	Time/node (ms)
PGEXPLAINER	0.41	0.62	0.38	Tree-Cycles	871	1,950	2.23	60.56
GEM	0.16	0.73	8.64	Tree-Grid	1,231	3,410	2.77	13.67
CF-GNNEX	1295.66	2382.51	3964.36	BA-Shapes	700	4,100	5.86	89.91
CF ²	165.56	249.92	2565.87	ogbn-arxiv	169,343	1,166,243	6.89	353.43
INDUCE (ind.)	4.36	17.64	68.33	Amazon-photos	7,487	119,043	15.90	5242.32
INDUCE (trans.)	66.08	331.58	6546.48					

(a) Efficiency

(b) Scalability

Table 6: (a) Running times (in seconds) of each algorithm on entire test set. (b) Scalability against various graph properties.



(a) Tree-Cycles

(b) Impact of additions

Figure 4: Visualization of counterfactual explanations for the same node (orange) produced by different methods. Semantically, the node label should flip if it is not a part of the motif. (a) Counterfactual explanation for Tree-Cycles Dataset, (b) Counterfactuals predicted by INDUCE.

explanations on unseen nodes. The proposed features not only lead to better explanations but also provide a significant speed-up allowing INDUCE to perform counterfactual analysis at scale.

Limitations: INDUCE performs counter-factual reasoning by perturbing only the topological space. In future, we will consider characterization of the node feature space and explore the joint combinatorial space of topology and features.

References

- [1] Carlo Abrate and Francesco Bonchi. Counterfactual graphs for explainable classification of brain networks. In *KDD*, page 2495–2504, 2021.
- [2] Steve Azzolin, Antonio Longa, Pietro Barbiero, Pietro Lio, and Andrea Passerini. Global explainability of GNNs via logic combination of learned concepts. In *The Eleventh International Conference on Learning Representations*, 2023.
- [3] Davide Bacciu and Danilo Numeroso. Explaining deep graph networks via input perturbation. *IEEE Transactions on Neural Networks and Learning Systems*, pages 1–12, 2022.
- [4] Mohit Bajaj, Lingyang Chu, Zi Yu Xue, Jian Pei, Lanjun Wang, Peter Cho-Ho Lam, and Yong Zhang. Robust counterfactual explanations on graph neural networks. In A. Beygelzimer, Y. Dauphin, P. Liang, and J. Wortman Vaughan, editors, *Advances in Neural Information Processing Systems*, 2021.
- [5] Uriel Feige. A threshold of $\ln n$ for approximating set cover. *Journal of the ACM (JACM)*, 45(4):634–652, 1998.
- [6] Matthias Fey and Jan Eric Lenssen. Fast graph representation learning with pytorch geometric. *arXiv preprint arXiv:1903.02428*, 2019.
- [7] Qiang Huang, Makoto Yamada, Yuan Tian, Dinesh Singh, and Yi Chang. Graphlime: Local interpretable model explanations for graph neural networks. *IEEE Transactions on Knowledge and Data Engineering*, 2022.
- [8] Mingjian Jiang, Zhen Li, Shugang Zhang, Shuang Wang, Xiaofeng Wang, Qing Yuan, and Zhiqiang Wei. Drug–target affinity prediction using graph neural network and contact maps. *RSC advances*, 10(35):20701–20712, 2020.

- [9] Jeroen Kazius, Ross McGuire, and Roberta Bursi. Derivation and validation of toxicophores for mutagenicity prediction. *Journal of medicinal chemistry*, 48(1):312–320, 2005.
- [10] Elias Khalil, Hanjun Dai, Yuyu Zhang, Bistra Dilkina, and Le Song. Learning combinatorial optimization algorithms over graphs. *Advances in neural information processing systems*, 30, 2017.
- [11] Thomas N Kipf and Max Welling. Semi-supervised classification with graph convolutional networks. *arXiv preprint arXiv:1609.02907*, 2016.
- [12] Wanyu Lin, Hao Lan, and Baochun Li. Generative causal explanations for graph neural networks. In *International Conference on Machine Learning*, pages 6666–6679. PMLR, 2021.
- [13] Ana Lucic, Maartje A Ter Hoeve, Gabriele Tolomei, Maarten De Rijke, and Fabrizio Silvestri. Cf-gnnexplainer: Counterfactual explanations for graph neural networks. In *AISTATS*, pages 4499–4511, 2022.
- [14] Dongsheng Luo, Wei Cheng, Dongkuan Xu, Wenchao Yu, Bo Zong, Haifeng Chen, and Xiang Zhang. Parameterized explainer for graph neural network. *Advances in neural information processing systems*, 33:19620–19631, 2020.
- [15] Tomas Mikolov, Ilya Sutskever, Kai Chen, Greg S Corrado, and Jeff Dean. Distributed representations of words and phrases and their compositionality. In C.J. Burges, L. Bottou, M. Welling, Z. Ghahramani, and K.Q. Weinberger, editors, *Advances in Neural Information Processing Systems*, volume 26. Curran Associates, Inc., 2013.
- [16] Azalia Mirhoseini, Anna Goldie, Mustafa Yazgan, Joe W. J. Jiang, Ebrahim M. Songhori, Shen Wang, Young-Joon Lee, Eric Johnson, Omkar Pathak, Sungmin Bae, Azade Nazi, Jiwoo Pak, Andy Tong, Kavya Srinivasa, William Hang, Emre Tuncer, Anand Babu, Quoc V. Le, James Laudon, Richard Ho, Roger Carpenter, and Jeff Dean. Chip placement with deep reinforcement learning. *CoRR*, abs/2004.10746, 2020.
- [17] Michael Sejr Schlichtkrull, Nicola De Cao, and Ivan Titov. Interpreting graph neural networks for nlp with differentiable edge masking. *arXiv preprint arXiv:2010.00577*, 2020.
- [18] Caihua Shan, Yifei Shen, Yao Zhang, Xiang Li, and Dongsheng Li. Reinforcement learning enhanced explainer for graph neural networks. In *NeurIPS 2021*, December 2021.
- [19] Oleksandr Shchur, Maximilian Mumme, Aleksandar Bojchevski, and Stephan Günnemann. Pitfalls of graph neural network evaluation. *arXiv preprint arXiv:1811.05868*, 2018.
- [20] Jonathan M Stokes, Kevin Yang, Kyle Swanson, Wengong Jin, Andres Cubillos-Ruiz, Nina M Donghia, Craig R MacNair, Shawn French, Lindsey A Carfrae, Zohar Bloom-Ackermann, et al. A deep learning approach to antibiotic discovery. *Cell*, 180(4):688–702, 2020.
- [21] Juntao Tan, Shijie Geng, Zuohui Fu, Yingqiang Ge, Shuyuan Xu, Yunqi Li, and Yongfeng Zhang. Learning and evaluating graph neural network explanations based on counterfactual and factual reasoning. In *Proceedings of the ACM Web Conference 2022*, WWW '22, page 1018–1027, 2022.
- [22] Petar Veličković, Guillem Cucurull, Arantxa Casanova, Adriana Romero, Pietro Liò, and Yoshua Bengio. Graph attention networks. In *International Conference on Learning Representations*, 2018.
- [23] Paul Voigt and Axel Von dem Bussche. The eu general data protection regulation (gdpr). *A Practical Guide, 1st Ed.*, Cham: Springer International Publishing, 10(3152676):10–5555, 2017.
- [24] Minh N Vu and My T Thai. Pgm-explainer: Probabilistic graphical model explanations for graph neural networks. *arXiv preprint arXiv:2010.05788*, 2020.
- [25] Kuansan Wang, Zhihong Shen, Chiyuan Huang, Chieh-Han Wu, Yuxiao Dong, and Anshul Kanakia. Microsoft Academic Graph: When experts are not enough. *Quantitative Science Studies*, 1(1):396–413, 2020.

- [26] Xiang Wang, Yingxin Wu, An Zhang, Xiangnan He, and Tat-seng Chua. Causal screening to interpret graph neural networks. 2021.
- [27] Geemi P Wellawatte, Aditi Seshadri, and Andrew D White. Model agnostic generation of counterfactual explanations for molecules. *Chemical science*, 13(13):3697–3705, 2022.
- [28] Ronald J. Williams. Simple statistical gradient-following algorithms for connectionist reinforcement learning. *Mach. Learn.*, 8(3–4):229–256, may 1992.
- [29] Jiacheng Xiong, Zhaoping Xiong, Kaixian Chen, Hualiang Jiang, and Mingyue Zheng. Graph neural networks for automated de novo drug design. *Drug Discovery Today*, 26(6):1382–1393, 2021.
- [30] Han Xuanyuan, Pietro Barbiero, Dobrik Georgiev, Lucie Charlotte Magister, and Pietro Lió. Global concept-based interpretability for graph neural networks via neuron analysis. 2023.
- [31] Rex Ying, Ruining He, Kaifeng Chen, Pong Eksombatchai, William L. Hamilton, and Jure Leskovec. Graph convolutional neural networks for web-scale recommender systems. In *KDD*, page 974–983, 2018.
- [32] Zhitao Ying, Dylan Bourgeois, Jiaxuan You, Marinka Zitnik, and Jure Leskovec. Gnnexplainer: Generating explanations for graph neural networks. *Advances in neural information processing systems*, 32, 2019.
- [33] Hao Yuan, Jiliang Tang, Xia Hu, and Shuiwang Ji. Xgnn: Towards model-level explanations of graph neural networks. In *Proceedings of the 26th ACM SIGKDD International Conference on Knowledge Discovery & Data Mining*, pages 430–438, 2020.
- [34] Hao Yuan, Jiliang Tang, Xia Hu, and Shuiwang Ji. Xgnn: Towards model-level explanations of graph neural networks. In *Proceedings of the 26th ACM SIGKDD International Conference on Knowledge Discovery & Data Mining (KDD)*, pages 430–438, 2020.
- [35] Hao Yuan, Haiyang Yu, Shurui Gui, and Shuiwang Ji. Explainability in graph neural networks: A taxonomic survey. *IEEE Transactions on Pattern Analysis and Machine Intelligence*, 2022.
- [36] Hao Yuan, Haiyang Yu, Jie Wang, Kang Li, and Shuiwang Ji. On explainability of graph neural networks via subgraph explorations. In *ICML*, pages 12241–12252. PMLR, 2021.

Method	Explainability Paradigm	Additions	Deletions	Inductive	# explainers required
GNNEXPLAINER[32]	Factual	X	✓	X	N
GRAPHMASK[17]	Factual	X	✓	X	N
CAUSAL SCREENING[26]	Factual	X	✓	X	N
SUBGRAPHX[36]	Factual	X	✓	X	N
PGM-EXPLAINER[24]	Factual	X	✓	X	N
PGEXPLAINER[14]	Factual	X	✓	✓	1
GEM[12]	Counterfactual	X	✓	✓	1
CF-GNNEXPLAINER[13]	Counterfactual	X	✓	X	N
CF ² [21]	Counterfactual + Factual	X	✓	X	N
INDUCE (OURS)	Counterfactual	✓	✓	✓	1

Table G: Comparison on properties of common perturbation-based GNN explainers. The last column shows the number of required explainers for a graph with N nodes.

Dataset	k-hop	#additions	#deletions	ratio (#additions/#deletions)
Tree-cycles	4	18313	1105	16.57
Tree-grid	4	98942	3960	24.98
BA-shapes	4	3140886	47580	66.01
Amazon-Photos	4	12144800	432160	28.10
ogbg-arxiv	3	354496362	524330	676.09

Table H: Ratio of no. of additions to deletions of datasets.

Appendix

A Proof of Theorem 1

PROOF. To prove NP-hardness of the problem we reduce it from the classical *set cover* problem.

Definition 1 (Set Cover [5]) Given a collection of subsets $\mathcal{S} = \{S_1, \dots, S_m\}$ from a universe of items $U = \{u_1, \dots, u_n\}$ identify the smallest collection of subsets $\mathcal{A}^* \subseteq \mathcal{S}$ covering the set U , i.e.,

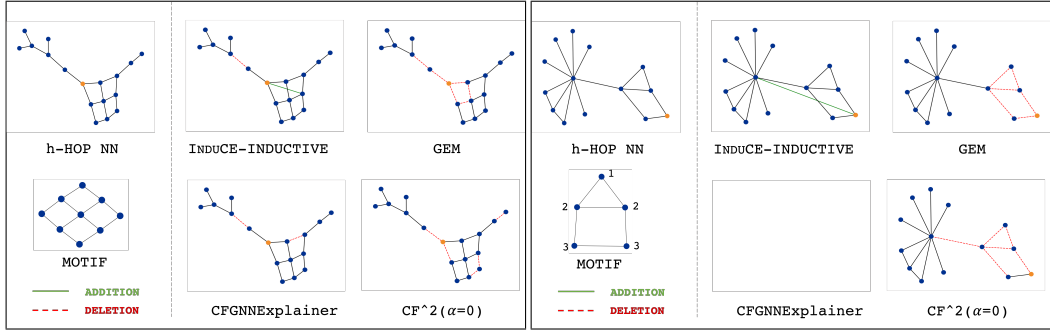
$$\mathcal{A}^* = \arg \min_{|\mathcal{A}|, \mathcal{A} \subseteq \mathcal{S}} \bigcup_{S_i \in \mathcal{A}} S_i = U \quad (14)$$

We show that given any instance of a set cover problem $\langle \mathcal{S}, U \rangle$, it can be mapped to Prob. 1. Specifically, we construct a graph $\mathcal{G} = (\mathcal{V}, \mathcal{E})$, where $\mathcal{V} = N \cup \mathcal{S} \cup U$. Here, N is an arbitrary set of nodes. In addition, we have a node corresponding to each set $S \in \mathcal{S}$ and each item $u \in U$. There is an edge between two nodes $v_i, v_j \in \mathcal{V}$ if v_i corresponds to some set $S \in \mathcal{S}$, v_j corresponds to item $u \in U$, and $u \in S$. There are no edges among nodes in N . The GNN Φ predicts the label of any node $v \in N$ as 1 if all nodes from U are reachable from v , otherwise 0. Furthermore, let the set of allowed perturbations be $\mathcal{V}_c = \{(v_i, v_j) \mid v_i \in N, v_j \in \mathcal{S}\}$. Given any $v \in N$, with $L_\Phi(\mathcal{G}, v) = 0$, the counterfactual reasoner therefore needs to identify the minimum number of edges to add so that all nodes from U are reachable from v through some nodes in \mathcal{S} .

With this construction, only edge additions are allowed. Now it is easy to see that the smallest edge set flipping the label of v corresponds to connecting v to nodes in \mathcal{A}^* , where \mathcal{A}^* is the solution for the set cover problem. \square

B Discounted Rewards

The objective of the policy Π is to find minimal counterfactual explanations for GNNs using the reward function mentioned in Eq 10. However, we can observe that in that equation, the marginal reward at each step is given equal weight. In our case, we want the immediate rewards to have higher weight over the rewards encountered later on in the perturbation trajectory \mathcal{T}_v in order to penalize larger counterfactual size, thus we use discounted rewards (Eq 15) with γ being the discount factor to achieve the objective. Since we want minimal explanation size, we use small values of γ (Refer App. F.3).



(a) Tree-Grid (b) BA-Shapes
 Figure E: Visualization of counterfactual explanations for the same node (orange) produced by different methods. Semantically, the node label should flip if it is not a part of the motif, i.e., (a) 3×3 -grid, and the (b) the house respectively. CF-GNNEXPLAINER is unable to find a counterfactual in (b).

Algorithm 1 Training pipeline of INDUCE.

Input: Graph \mathcal{G} , GNN Φ , Train set \mathcal{V}_{tr} , perturbation budget δ , number of episodes M

Output: Policy Π

```

1:  $\mathcal{V}_{batch} \leftarrow \{\mathcal{V}_1, \mathcal{V}_2, \dots, \mathcal{V}_B \mid \cup_{i=1}^B \mathcal{V}_i = \mathcal{V}_{tr}\}$  ▷ Random partitioning instances of  $\mathcal{V}_{tr}$  into  $B$  batches
2:  $\Pi \leftarrow$  initialize with random parameters
3: for all  $e \in [1, M]$  do
4:   for all  $\mathcal{V}_b \in \mathcal{V}_{batch}$  do
5:     for all  $v \in \mathcal{V}_b$  do
6:        $t \leftarrow 0$ 
7:       while  $L_\Phi(\mathcal{G}^0, v) = L_\Phi(\mathcal{G}^t, v)$  &  $t < \delta$  do
8:         compute  $\mathcal{S}_v^t$ 
9:          $a^t \leftarrow$  sample from  $\Pi(\mathcal{S}_v^t, \mathcal{P}^t)$ 
10:         $\mathcal{G}_v^{t+1} \leftarrow$  perturb  $\mathcal{G}_v^t$  with edge  $a^t$ 
11:         $\mathcal{R}_v^t \leftarrow$  compute reward using Eq.10
12:         $\mathcal{R}_{dis,v}^t \leftarrow$  compute discounted rewards using Eq.15
13:         $\tilde{\mathcal{R}}_{dis,v}^t \leftarrow$  normalize discounted rewards using Eq.16
14:         $t \leftarrow t + 1$ 
15:       Backpropagate to minimize loss using Eq. 17
16: Return  $\Pi$ 

```

$$\mathcal{R}_{dis,v}^t(a_t) = \sum_{i=0}^{\delta} \gamma^i \mathcal{R}_v^{t+i+1}(a_t) \quad (15)$$

here δ is the maximum perturbation budget.

One limitation of policy gradient is high variance caused by the scale of rewards. A common way to reduce variance is to subtract a baseline, $b(\mathcal{S}_v^t)$ such that it does not induce bias in the policy gradient. A simple baseline can be the mean of the discounted rewards, so that we train the policy to pick trajectories that give rewards better than the average rewards. We also normalize the discounted reward further by dividing with the standard deviation.

$$\tilde{\mathcal{R}}_{dis,v}^t(a_t) = \frac{\mathcal{R}_{dis,v}^t(a_t) - \bar{\mathcal{R}}_{dis,v}^t(a_t)}{\max(\sigma(\mathcal{R}_{dis,v}^t(a_t)), c)} \quad (16)$$

where $\sigma(\mathcal{R}_{dis}^t)$ is the standard deviation, c is a constant. The optimized version of the loss function(Eq 12) is in App. C.

C Batching

Equation 12 takes an average gradient over all examples in the training set. This setting may lead to over-smoothing of the gradients and hence induce difficulty in training. To counter this issue, we performed batching of node instances, and back-propagated with the average gradients computed on nodes in the batch. Thus we optimize our policy on batches of nodes, and use normalized discounted rewards in the loss function(Refer Eq. 17).

Algorithm 2 Test pipeline of INDUCE.

Input: Graph \mathcal{G} , GNN Φ , Test set \mathcal{V}_{test} , maximum perturbation budget δ **Output:** Counterfactual explanations CF

```
1:  $CF = \phi$ 
2:  $\Pi \leftarrow$  parameters of pre-trained policy
3: for all  $v \in \mathcal{V}_{test}$  do
4:    $Exp \leftarrow \emptyset$ 
5:    $t \leftarrow 0$ 
6:   while  $L_\Phi(\mathcal{G}^0, v) = L_\Phi(\mathcal{G}^t, v)$  &  $t < \delta$  do
7:     compute  $\mathcal{S}_v^t$ 
8:      $a^* \leftarrow \arg \max_{a \in \mathcal{P}^t} \Pi(\mathcal{S}_v^t, \mathcal{P}^t)$ 
9:      $\mathcal{G}_v^{t+1} \leftarrow$  perturb  $\mathcal{G}_v^t$  with edge  $a^*$ 
10:     $t \leftarrow t + 1$ 
11:   if  $L_\Phi(\mathcal{G}^0, v) \neq L_\Phi(\mathcal{G}^t, v)$  then
12:      $CF = CF \cup Exp$ 
13: Return CF
```

Dataset	Train accuracy(%)	Test Accuracy(%)
Tree-cycles	91.23	90.86
Tree-grid	84.34	87.44
BA-shapes	96.61	98.57
Amazon-Photos	89.59	88.75
ogbn-arxiv	71.59	55.07

Table I: Accuracy of GNN Φ on the three benchmark datasets.

$$\mathcal{J}(\Pi) = -\frac{1}{V_{batch}} \left(\sum_{v \in V_{batch}} \left(\sum_{t=0}^{|\mathcal{T}_v|} \log p_{a,v}^t \tilde{\mathcal{R}}_{dis,v}^t(a_t) + \eta Ent(\mathcal{P}_v^t) \right) \right) \quad (17)$$

D INDUCE: Algorithm

The training and test pipelines of INDUCE are provided in Alg. 1 and Alg. 2 respectively. As evident from Alg. 2, using INDUCE we can train once and test on unseen nodes using just a forward pass through the policy network which makes it more efficient than the transductive baselines (recall Table 6a).

E Complexity of INDUCE

Train-Phase: Training the policy network involves four key steps, i.e., compute the state, forward pass through the policy network, sample and take action, and compute the marginal reward of the action. Among the above, state computation and performing the action take $\mathcal{O}(1)$ time. Time taken by a forward pass through the policy network involves a combination of computing node embeddings using GAT and computing a score for each action in the action space \mathcal{P}^t through the MLP. Forward pass through the GAT takes $\mathcal{O}(K(|\mathcal{V}|h_i h_d + |\mathcal{E}|h_d))$ [22] where K , h_i and h_d are the number of GAT layers, input and hidden dimensions respectively. Action score computation using MLP takes $\mathcal{O}(|\mathcal{P}^t|h_m(h_d + (J - 2)h_m + 1))$, J and h_m are number of MLP layers and hidden dimensions. Computing the reward function involves taking a forward pass through a GCN which takes $\mathcal{O}(L|\mathcal{E}|h_i h_d |\mathcal{C}|)$ time, here L and $|\mathcal{C}|$ are the number of layers and number of classes respectively. The above steps are repeated for M episodes for each node in training set V_{tr} until a maximum of δ time steps. Combining the above costs, treating J , K , L , h_i , h_d , h_m and $|\mathcal{C}|$ as fixed constants which have small values, and with the knowledge that $|\mathcal{P}^t| = \mathcal{O}(|\mathcal{V}| + |\mathcal{E}|)$ (refer Eq. 6), the complexity with respect to the input parameters reduces to $\mathcal{O}(|V_{tr}|M\delta(|\mathcal{V}| + |\mathcal{E}|))$.

Test-Phase: The test phase involves state computation, forward pass through the policy network, and performing the action with highest probability for a maximum of δ time-steps for

every node in the test set \mathcal{V}_{test} . Therefore following the discussion in the training phase, the time complexity of test phase is $\mathcal{O}(|\mathcal{V}|_{test}|\delta(|\mathcal{V}| + |\mathcal{E}|)|)$.

Detailed algorithm of INDUCE is given in App. D.

F Experimental Setup

All reported experiments are conducted on an NVIDIA DGX Station with four V100 GPU cards having 128GB GPU memory, 256GB RAM, and a 20 core Intel Xeon E5-2698 v4 2.2 Ghz CPU running in Ubuntu 18.04.

F.1 Benchmark datasets

- **BA-SHAPES:** The base graph is a Barabasi-Albert (BA) graph. The motifs are **house-shaped** structures made up of 5 nodes (Refer Figure Eb). Non-motif nodes are assigned class 0, while nodes at the top, middle, and bottom of the motif are assigned classes 1, 2, and 3, respectively.
- **TREE-CYCLES:** The base graph is a binary tree with **6-node cycles** used as motifs (Refer Figure 4a). The motifs are connected to random nodes in the tree. Non-motif nodes are labelled 0, while the motif nodes are labelled 1.
- **TREE-GRID:** The base graph is a binary tree and the motif is a **3 × 3 grid** connected to random tree nodes (Refer Figure Ea). Just like tree-cycles dataset binary class labelling has been done.

F.2 Baselines

- **CF-GNNEXPLAINER** [13]: Being a transductive method for counterfactual explanations, it learns a new set of parameters for every node and cannot be used to explain unseen nodes.
- **CF²** [21]: While being transductive in nature, it combines both counterfactual and factual properties to give an explanation. CF² tunes the parameter α to weigh the contribution of factual explanations. We compare CF² with $\alpha = 0$ where it becomes as a counterfactual explainer.
- **GEM** [12]: This is inductive by nature, however, it only considers edge deletions. It has a limitation that it learns a counterfactual explanation model where the number of perturbations is fixed, i.e., it does not minimize the number of perturbations with the sole focus on flipping the label. We use the default size of 6 as the perturbation size as recommended by the authors. Note that GEM is not extendable to include edge additions. Specifically, GEM has a distillation process that generates the ground truth. Distillation involves removing every edge in a node’s neighbourhood iteratively and seeing its effect on the loss. The deletions are then sorted based on their effect on the loss. The top- k edges (k is user-specified) are used as the distilled ground truth. The explainer is later trained to generate graphs that are the same as the distilled ground truth. To extend this process for additions, the number of possible edge edits is significantly higher and the iterative process of GEM to create the distilled ground truth does not scale. In addition, it is also unclear how to set k in the presence of additions.
- **PGEXPLAINER** [14]: This method is also inductive and only considers edge deletions. It is a factual explainability method and requires a fixed explanation size as a hyper-parameter. We use the default size of 6 as the perturbation size as recommended by the authors for the benchmark datasets. We also use size 6 and 4 for Amazon-Photos and ogbn-arxiv, respectively.
- **RANDOM:** We use the same baseline as used in [13]. It makes the choices of deleting an edge randomly by generating a random subgraph mask for the h -hop neighbourhood of the node and perturbing it.

F.3 Training and Parameters

Counter-factual task: We provide a node that is part of a motif to the counterfactual explainer, and the task is to flip its label by recommending changes in the graph. All nodes that are part of a motif, are given a specific label and non-motif nodes are given a different label. Since the nodes are always chosen from motifs, the explanation is the motif itself. This setup is identical to CF² and CF-GNNEXPLAINER.

The GNN model Φ : We use the same GNN model used in CF-GNNEXPLAINER and CF². Specifically, it is a Graph Convolutional Networks trained on each of the datasets. Each model has 3 graph convolutional layers, with 20, 128 and 256 hidden dimensions for the benchmarking datasets,

Amazon-photos and ogbn-arxiv respectively. The non-linearity used is *relu* for the first two layers and *log SoftMax* after the last layer of GCN. The learning rate is 0.01. The train and test data are divided in the ratio 80:20 for benchmark datasets. For ogbn-arxiv, we use the standard splits provided in the ogb package. In our experiments, we use a scaled-down version of the Amazon-Photos dataset. We choose one random node as the central node and took its 3-hop neighbourhood in our dataset. Amazon Photos has an average degree of 13, hence, the 3-hop neighborhood covers a reasonable distribution of class labels. We split the nodes of this subgraph in the ratio of 80 : 20 for train and test sets. The accuracy of the GNN model Φ for each dataset is mentioned in Table I.

Training, Inference and Parameters: For INDUCE and GEM, we use a train/evaluation split of 80/20 on the benchmark and the Amazon-Photos datasets. For ogbn-arxiv, we train on 10 random examples per class, and sample 1000 random nodes as the test dataset. We make sure that the test and train sets are disjoint. The evaluation set for all techniques are identical. For GEM and INDUCE, the train set is identical. Since CF-GNNEXPLAINER and CF² are transductive, only the evaluation set is used for them where they learn a node-specific parameter set. The same happens on the transductive version of INDUCE.

Parameters settings: We use $h = 4$ because extracting the 4-hop neighbourhood as the subgraph ensured that we preserve the black-box model’s accuracy. We use $\beta = 0.5$ so as to give equal weight to the predict loss and distance loss (see Eq. 10). We use different values of $\gamma \in \{0.4, 0.6\}$ and find the best performance at $\gamma = 0.4$ for the inductive setting and $\gamma = 0.6$ for the transductive setting with a maximum perturbation budget $\delta = 15$. We use maximum number of episodes $\mathbb{M} = 80, 500, 500$ for BA-shapes, Tree-cycles and Tree-grid respectively. We use GAT as the GNN of choice for the policy network. For the policy network, we use 3 GAT layers, 2 fully connected MLP layers, 16 hidden dimension, a learning rate of .0003 and LeakyReLU with negative slope 0.1 as the activation function. We use three different values for $\eta \in \{0.1, 0.01, 0.001\}$ and $\eta = 0.1$ improves the performance due to higher weight for exploration.

Method	Sparsity (Tree-Cycles)	Sparsity (Tree-Grid)	Sparsity (BA-Shapes)	Amazon-photos	ogbn-arxiv
CF-GNNEXPLAINER	0.93	0.95	0.99	NULL	DNS
CF ²	0.52	0.59	0.92	0.99	DNS
INDUCE- transductive	0.92	0.96	0.98	0.99	0.78

Table J: Comparison of "sparsity" of counterfactuals predicted by transductive methods. "NULL" means the baseline could not find a counterfactual. "DNS" means that the baseline did not scale.

Method	Sparsity (Tree-Cycles)	Sparsity (Tree-Grid)	Sparsity (BA-Shapes)	Amazon-photos	ogbn-arxiv
PGEXPLAINER	0.34	0.64	0.61	NULL	0.66
GEM	0.54	0.77	0.88	NULL	DNS
INDUCE- inductive	0.81	0.83	0.98	0.99	0.64

Table K: Comparison of "sparsity" of counterfactuals predicted by inductive methods. "NULL" means the baseline could not find a counterfactual. "DNS" means that the baseline did not scale.

G Additional Results on Sparsity of Counterfactuals

Recall, sparsity is defined as the proportion of edges in \mathcal{N}_v^ℓ , i.e., the ℓ -hop neighbourhood of the target node v . Since counterfactuals are supposed to be minimal, a value close to 1 is desired. We compare INDUCE with its baselines on sparsity in Tables J and K. We observe that INDUCE produces

Policy Variant	Tree-Cycles		
	Fid.(%) ↓	Size ↓	Acc.(%) ↑
INDUCE-inductive-GCN	0	2.62 ±1.52	78.84
INDUCE-inductive-GAT	0	1.99 ±1.00	97.47
INDUCE-transductive-GCN	0	1.08 ±0.27	96.84
INDUCE-transductive-GAT	0	1.08 ±0.27	96.20

Table L: Importance of attention in the GNN component of INDUCE.

Method	Tree-Cycles			Tree-Grid			BA-Shapes		
	Fid.(%) ↓	Size ↓	Acc.(%) ↑	Fid.(%) ↓	Size ↓	Acc.(%) ↑	Fid.(%) ↓	Size ↓	Acc.(%) ↑
Features only	0	3.12 ±1.96	80.05	0	4.50 ±3.16	73.12	18.4	3.62 ±3.46	70.29
Features + D	0	2.56 ±1.73	65.74	0	3.71 ±2.51	84.26	9.2	4.02 ±4.27	98.89
Features + E	0	2.24 ±1.15	72.69	0	3.37 ±2.22	94.63	68.4	1.25 ±0.83	86.25
Features + OH	0	3.19 ±1.83	79.70	2.3	4.10 ±3.13	87.17	28.9	4.63 ±3.41	32.75
Features + D + E	0	2.81 ±1.55	85.19	0	3.12 ±1.96	84.77	48.7	2.43 ±2.65	63.71
Features + D + OH	0	2.65 ±1.58	69.31	0	3.16 ±2.21	92.02	1.3	3.62 ±2.45	62.08
Features + E + OH	0	2.62 ±1.52	78.84	0	3.47 ±2.28	89.15	27.6	4.2 ±3.02	56.00
Features + D + E + OH	0	2.31 ±1.44	96.65	0	4.67 ±2.91	91.05	2.6	4.37 ±3.53	64.4

Table M: Ablation study results. D, E, and OH represents degree, entropy, and one hot encoded labels respectively. We vary node features along with different heuristic features to measure the effect of each of these features. Our proposed method INDUCE is superior when it uses all the features.

better or comparable explanations in terms of sparsity. In Table K we observe that the sparsity of INDUCE-inductive is slightly less than PGEXPLAINER for the ogbn-arxiv dataset. However, the fidelity of PGEXPLAINER is greater than INDUCE-inductive (Recall Table 5b). Thus, when looking at the combined results, one may conclude that PGEXPLAINER finds counterfactual explanations for the easier examples and, as a result, has sparser explanations. Similarly, we can interpret the sparsity of CF-GNNEXPLAINER being better than INDUCE-transductive for Tree-Cycles in Table J as its fidelity is much higher than the latter (Recall Table 2).]

H Ablation Study

To infuse more information about the local graph structure and its statistics, we use several heuristic features such as degree, entropy, and one-hot encoded labels (Refer 3.1). We conduct an ablation study to investigate the effectiveness of each heuristic feature. Table M summarises the findings. Our method is most consistent when it uses all features. Note that *features* and *entropy* together produce competitive results. However, the fidelity in BA-Shapes becomes much worse from this combination. This means, in most of the cases, this combination is unable to find the counterfactual example. In such cases, the possibility of getting better values in other measures increases.

GCN Vs. GAT: INDUCE uses a GAT to train the RL policy. In the next experiment, we evaluate the impact of replacing the GAT with a Graph Convolutional Network (GCN). The results are presented in Table L. We see that GAT significantly outperforms GCN in the inductive version and thereby justifying our choice.

Heuristic Features: Table M contains an exhaustive analyses of the performance of INDUCE-INDUCTIVE using all combinations of heuristic features mentioned in section 3. The combination of features and entropy seems to allow best performance of the model on Tree-grid and Tree-cycles datasets, however as we see in Table 1 that BA-shapes is a dense network and clearly the degree heuristic in combination with node features leads to excellent performance for BA-shapes in terms of the size and the accuracy. Since the ability of the method to find a counterfactual weighs more, our default model containing all heuristic combined with node features gives best overall performance in fidelity, with size and accuracy being better or comparable to the other combinations in most cases.

I Additional Results on Counterfactual Size Distributions

In figures F and G we observe the distributions of edit distance between the original and the counterfactual h -hop neighbourhood of instances in Tree-Grid and BA-Shapes datasets respectively. As observed both in inductive and transductive versions of INDUCE most of the counterfactuals are of small size and dominated by edge additions. However, we can also observe that the transductive versions of INDUCE does produce counterfactuals of size mostly localised around 1. This is because the parameters are tailored instance by instance. INDUCE-inductive however with a minor trade-off in the counterfactual size, provides a comparable performance to INDUCE-transductive (recall Tables 2 and 3) while providing a speed-up of 79x over all the transductive baselines (recall Table 6a). We further conduct experiments on how the accuracy of the explainer is affected with increasing counterfactual size in App. J.

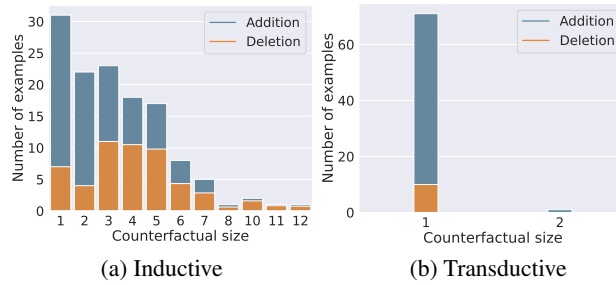


Figure F: The distributions of the edit size and their internal composition of edge additions and deletions by INDUCE on the Tree-Grid dataset.

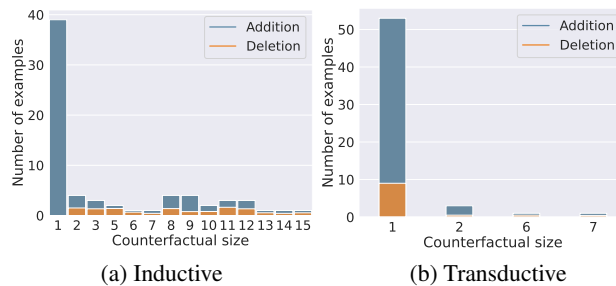


Figure G: The distributions of the edit size and their internal composition of edge additions and deletions by INDUCE on the BA-Shapes dataset.

J Size vs. Accuracy Trade-off

The accuracy vs. counterfactual size trade-off for Induce in Table N and O. We observe that with higher size, the accuracy decreases. Recall, we use benchmark datasets with ground-truth explanations where a node belongs to a particular class if it belongs to a certain motif. Hence, an explanation is accurate if it includes edges from the motif. We observe that when the explainer fails to find short explanations, it typically deviates towards a sequence of edges outside the motif. Hence the explainer fails to flip the label till a large set of edits are made.

Size	Acc. % (Tree-Cycles)	Acc. % (Tree-Grid)	Acc. % (BA-Shapes)
1	100	100	100
3	94	97	100
5	73	89	100
6	83	NA	NA
7	86	88	100
10	NA	80	100
15	NA	73	73

Table N: **Counterfactual Size vs. Accuracy Trade-off for INDUCE- inductive:** The results suggest that as counterfactual size increases, the accuracy of the explanation decreases. NA stands for counterfactual of that size was not present.

Size	Acc. % (Tree-Cycles)	Acc. % (Tree-Grid)	Acc. % (BA-Shapes)
1	97	98	100
2	100	100	100
6	NA	NA	50
7	NA	NA	57

Table O: **Counterfactual Size vs. Accuracy Trade-off for INDUCE- transductive:** The results suggest that as counterfactual size increases, the accuracy of the explanation decreases. NA stands for counterfactual of that size was not present.

K Baselines for “ogbn-arxiv” Dataset.

The baselines do not scale for Ogbn-arxiv dataset. We describe the details as follows. Ogbn-arxiv is a **million-sized** node prediction dataset with **169,343** nodes and **1,166,243** edges. CF² and GEM do not scale (Recall Tables 5a and 5b) on this dataset since they employ computations on a dense adjacency matrix, which require $\mathcal{O}(n^2)$ space, where n is the number of nodes in the graph. For a million-sized graph, this leads to memory overflow. Adapting to a sparse adjacency matrix requires non-trivial changes to the source code.

CF-GNNEXPLAINER extracts the k -hop neighbourhood of a target node at runtime and adapts to sparse adjacency matrices more easily. CF-GNNEXPLAINER’s algorithm is model-agnostic, however, the code-base is suitable for its customized black-box and cannot be trivially extended to any other black-box. The explainer loads the black-box weights into itself before freezing them, assuming that the black-box uses the same architecture as itself. It then uses those weights rather than the black-box GNN during the explanation. In case the explainer’s architecture does not match the black-box architecture, the keys for loading the weights do not match, hence, the explainer’s weights are not loaded, rather randomly initialized. As a result, the explainer gets initialized with random weights rather than the black-box’s weights and acts as a random classifier. This is an inefficient design choice and prevents CF-GNNEXPLAINER’s code from scaling for ogbn-arxiv (Recall Table 5a). We use PyTorch-geometric’s [6] standard *GCNConv* layers [11] that are compatible with sparse adjacency matrices to scale the black-box GNN to the million-sized graph. INDUCE’s code is written in a model-agnostic fashion. Any black-box GNN which employs *log SoftMax* non-linearity at the last layer is compatible with INDUCE.